Applied Surface Science 443 (2018) 68–73

Contents lists available at ScienceDirect

Applied Surface Science

journal homepage: www.elsevier.com/locate/apsusc

Full Length Article

Damage evaluation of proton irradiated titanium deuteride thin films to be used as neutron production targets

Manuel Suarez Anzorena [a,b], Alma A. Bertolo [a,b], Leonardo Gagetti [a,c], Pedro A. Gaviola [a,b], Mariela F. del Grosso [a,c,d,*], Andrés J. Kreiner [a,c,e]

[a] Gerencia de Investigación y Aplicaciones, Comisión Nacional de Energía Atómica, Av. Gral Paz 1499, B1650KNA San Martín, Buenos Aires, Argentina
[b] Instituto Sabato, Universidad Nacional de San Martín (UNSAM) – Comisión Nacional de Energía Atómica (CNEA), Buenos Aires, Argentina
[c] Consejo Nacional de Investigaciones Científicas y Técnológicas (CONICET), Rivadavia 1917, C1033AAJ Ciudad de Buenos Aires, Argentina
[d] GRUCAMM, Universidad Tecnológica Nacional Gral. Pacheco, H. Yrigoyen 288, B1617FRP, General Pacheco, Buenos Aires, Argentina
[e] Escuela de Ciencia y Tecnología, Universidad Nacional de San Martín (UNSAM), B1650HMQ San Martín, Buenos Aires, Argentina

ARTICLE INFO

Article history:
Received 3 January 2018
Revised 20 February 2018
Accepted 22 February 2018
Available online 23 February 2018

Keywords:
Titanium deuteride films
Neutron production targets
Irradiation
X-ray diffraction
LIBS
ERDA

ABSTRACT

Titanium deuteride thin films have been manufactured under different conditions specified by deuterium gas pressure, substrate temperature and time. The films were characterized by different techniques to evaluate the deuterium content and the homogeneity of such films. Samples with different concentrations of deuterium, including non deuterated samples, were irradiated with a 150 keV proton beam. Both deposits, pristine and irradiated, were characterized by optical profilometry and scanning electron microscopy.

1. Introduction

Research and development of neutron production targets through nuclear reactions, induced by charged particle beams provided by high power accelerators, can be used as a powerful tool in numerous fields where neutron beams are required. Some of those fields are: accelerator based boron neutron capture therapy (AB-BNCT) [1], homeland security, non-proliferation and in particular the accelerator driven systems (ADS) which are being developed to be used for the incineration of nuclear wastes throughout a transmutation process as well as for advanced application in the power generation [2,3], among many other medical and nuclear applications [4,5].

Neutron production targets are being studied around the world and in particular in Argentina as part of a project underway to develop high current accelerators for medical and nuclear applications [6]. One of the main characteristics of these targets will be the ability to withstand the radiation and hydrogen damage induced by the deuteron beam's high fluence [7]. In particular, when the D(d,n) reaction is considered, the development of TiD_2 targets is an important matter in the nuclear materials development and in neutron production.

Ti and TiD_2 thin films generation and characterization have been extensively studied and reported [8–10]. Irradiation of such films has been carried out using fluences of up to 1.2×10^{17} ions/cm^2 [11,12]. In this work, we show the results of the development of TiD_2 thin films and their behavior under proton irradiation with fluences of up to 3×10^{18} ions/cm^2. To study the irradiation damage, non irradiated and irradiated films were characterized by several techniques, and irradiation simulations were performed.

2. Materials and methods

In order to obtain TiD_2 thin films, Ti deposits were made using a physical vapor deposition (PVD) process on two different substrates: 1050 aluminum alloy and ETPHC copper, in the form of 3 mm thick discs. The substrates were previously polished up to 1 μm grit polishing cloth and cleaned in an ultrasonic bath for 15 min. Ti thin films were made with a substrate temperature of

* Corresponding author at: Gerencia de Investigación y Aplicaciones, Comisión Nacional de Energía Atómica, Av. Gral Paz 1499, B1650KNA San Martín, Buenos Aires, Argentina.
E-mail address: delgross@tandar.cnea.gov.ar (M.F. del Grosso).

https://doi.org/10.1016/j.apsusc.2018.02.222
0169-4332/

423 K and 523 K, for Cu and Al respectively, a pressure between 4 and 8 $\times 10^{-3}$ Pa and a deposition rate between 20–25 Å/s. Once the titanium film is deposited on the substrates, and without loosing vacuum inside the deposition chamber, the samples were impregnated with deuterium under controlled temperature, time and D_2 pressure conditions [10,13,14]. The deuterium pressure (P_{D_2}) varied between 0.1 $\times 10^5$ Pa, 0.5 $\times 10^5$ Pa and 1.0 $\times 10^5$ Pa, the substrate temperature (T_s) was taken within 373 K and 473 K, and the exposure time (t_e) was set among 0.5 h, 1 h and 2 h. Since deuterium concentration may not reach the stoichiometric relation of two deuteriums per each titanium, due to the inherent experimental performance, we will refer to it as TiD_x samples.

TiD_x films with the highest deuterium concentration, were irradiated at the ion injector of the TANDAR accelerator at National Atomic Energy Commission, Argentine, by a proton beam of 150 keV and currents between 3 and 12 μA, depending on ion source conditions. Beam diameters varied between 7 and 20 mm, which corresponded to current density of 9.5×10^{-4} mA/cm^2 and 3.1×10^{-2} mA/cm^2 respectively, reaching fluences up to 3×10^{18} ions/cm^2. In order to evaluate the temperature reached by the system, under the irradiation conditions, finite element simulations were carried out. For all cases, the simulations showed maximum temperatures of the samples below 363 K.

All samples were characterized by different techniques. Physical characterization includes the measurement of TiD_x film thickness with an optical profiler NT1100 (Veeco Instruments Inc.). Adhesion tests were carried out with the tape test technique [8], and surface micrographs were taken with an environmental scanning electron microscopy (ESEM) Quanta 200 (FEI Company), which includes an energy dispersive spectroscopy (EDS) Apollo X detector (EDAX Inc.). Crystallographic characterizations were performed by grazing incidence X-ray diffraction (GIXRD) Empyrean (PANalytical B.V.) with a PIXcel3D detector. Finally to determine the elemental composition of the samples we used two different techniques: laser induced breakdown spectroscopy (LIBS) that was carried out using a LIBS2500plus (Ocean Optics Inc.), the equipment has a 50 mJ Nd:YAG laser, a lens 25x60 NIRI (ACH-NIR) to focus the emitted light and a HR2000 + CCD [15]; and elastic recoil detection analysis (ERDA) [16], using a telescope detector (a solid state detector plus a gaseous type detector) and a TNT-N1728 (CAEN) multichannel analyzer for data acquisition. The use of a telescope detector allowed us to study the depth profile of deuterium and titanium at the same time. Data processing for the ERDA technique was performed using a MATLAB code, written specifically for this purpose.

The SRIM code [17] was used to calculate the beam range and the displacements per atom (DPA) caused by irradiation, using the recommended calculation method from Stoller et al. [18].

3. Results and discussion

3.1. Ti thin films

Well adhered Ti deposits on Cu and Al substrates were obtained, achieving mean roughness values between (11.09 ± 3.50) nm and (19.30 ± 4.00) nm and thicknesses between (1.89 ± 0.01) μm and (2.58 ± 0.01) μm. On Fig. 1 SEM micrographs can be seen: Fig. 1 (a) shows the granular surface morphology of the deposit and in Fig. 1(b) it can be observed a lateral view of the Ti film and a measure of its thickness.

3.2. Characterization of titanium deuteride films

SEM micrographs were made to characterize the surface morphology of the titanium deuteride films. As can be seen in Fig. 2, the titanium deuteride kept the same surface morphology of the titanium thin film, shown in Fig. 1. In order to study deuterium distribution and concentration in Ti thin films, all samples were analyzed with ERDA, LIBS and GIXRD. We were able to evaluate the homogeneity of the deuterium distribution, in the depth of the deposit by means of ERDA and across the surface by means of LIBS. The deuterium concentration and crystalline structure was evaluated by GIXRD. Also, by means of the previously mentioned techniques, we could find that a group of samples retained a higher deuterium concentration, while for other samples, the amount of deuterium retained was lower.

In Fig. 3 can be seen two different TiD_x samples measured with ERDA, (a) with low concentration of deuterium and (b) with a higher concentration. Regarding the relation between the deuterium and titanium counts we can find that the parameters that benefit the deuterium absorption are: $P_{D_2} = 1 \times 10^5$ Pa, T_s = 473 K and t_e = 0.5–2 h. It was observed that deuterium impregnation saturates after such times. The signal level of oxygen is due to the surface layer of TiO_2 generated by being in contact with the atmosphere, and the small signal levels of carbon indicate film contamination, that could either come from impurities present in the deposition chamber or simply from environmental pollution. On the other hand, substrate ions (Al or Cu) lose all their energy and do not reach the solid detector E, therefore they do not present events on these graphics. The concentration depth profile, for

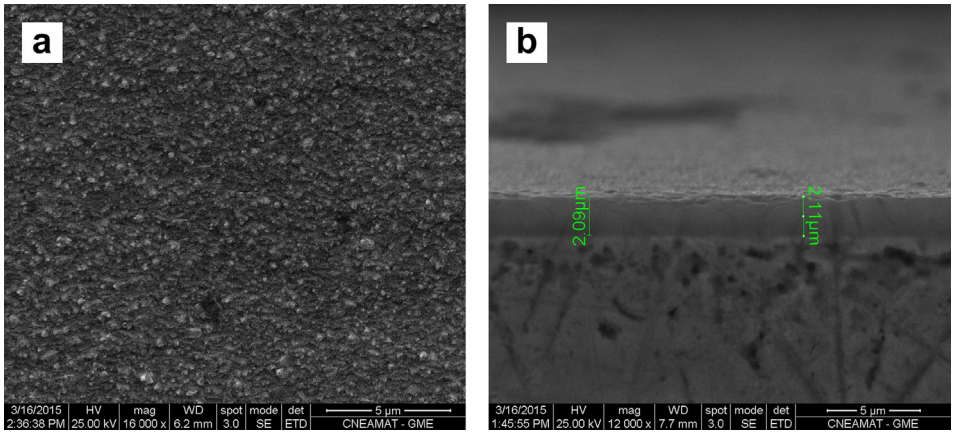

Fig. 1. SEM micrograph of (a) the surface and (b) a lateral view of a Ti deposit on a Cu substrate.

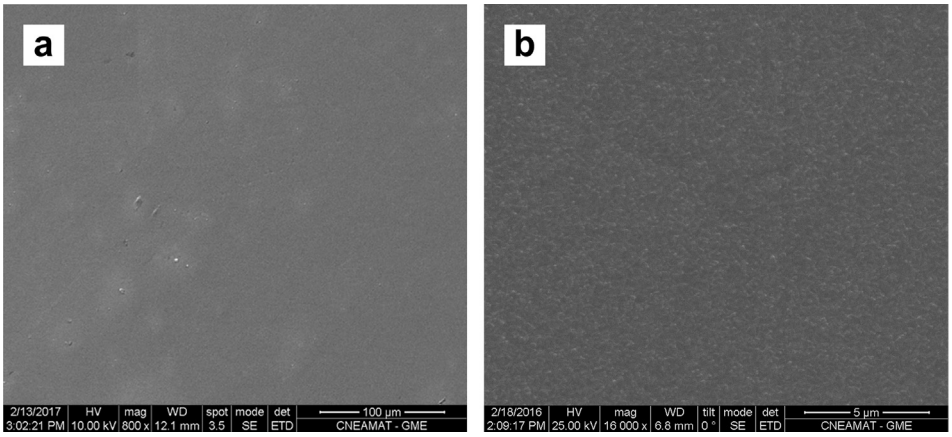

Fig. 2. SEM micrographs at two different magnifications of a titanium deuteride film surface, with deuterium absorption parameters $P_{D_2} = 1 \times 10^5$ Pa, T_s = 473 K and t_e = 2.0 h.

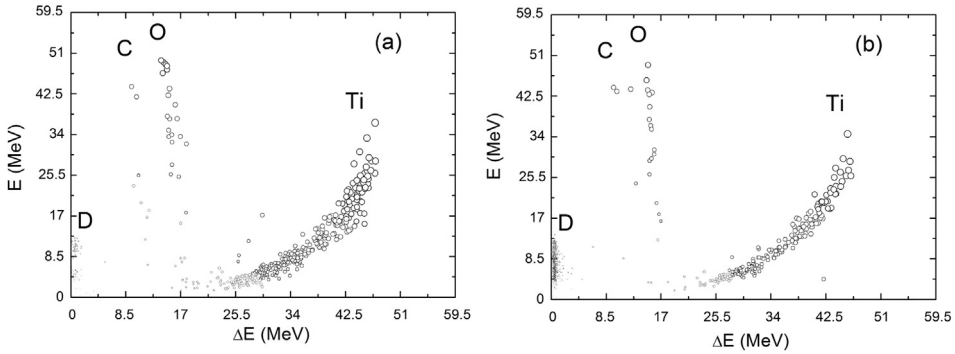

Fig. 3. E-ΔE spectrum of two TiD_x samples with (a) low concentration of D, made with $P_{D_2} = 1 \times 10^5$ Pa, T_s = 373 K and t_e = 1 h and (b) high concentration of D, made with $P_{D_2} = 1 \times 10^5$ Pa, T_s = 473 K and t_e = 2 h. Each bubble represents several scattering events, showing the areas with higher ion concentration.

samples with low (a) and high deuterium concentration (b) are shown in Fig. 4. The low concentration sample showed that deuterium is homogeneously distributed throughout the thickness of the titanium thin film while, in the other, there are a slight decrease in its amount inside the film.

A similar result was obtained by LIBS. Deuterium and titanium identification was made through 50 single shots throughout the surface of the samples. The spectrum lines located at 434.40 nm and 429.86 nm correspond to deuterium and titanium respectively. On Fig. 5 can be seen the intensity of the 434.40 nm spectrum line on different samples: a pure titanium sample that shows values with intensity near 0 at the bottom, conversely a sample with high deuterium content that exhibits an intensity above 0.5 (in arbitrary units) at the top part of the figure. The uniformity of the compound concentration throughout the surface was also checked due to the fairly constant intensity obtained along 50 shots.

The crystallography and phase composition of the samples were performed with GIXRD. The measurements were carried out at room temperature, with CuK_α radiation, under an incidence angle of 1° for the pure Ti samples and 3° for the TiD_x samples, in order to analyse the phases that are present inside the film more precisely. As an example, Fig. 6(a) shows X-ray diffractograms of a pure Ti thin film at the bottom and of a TiD_x sample with high

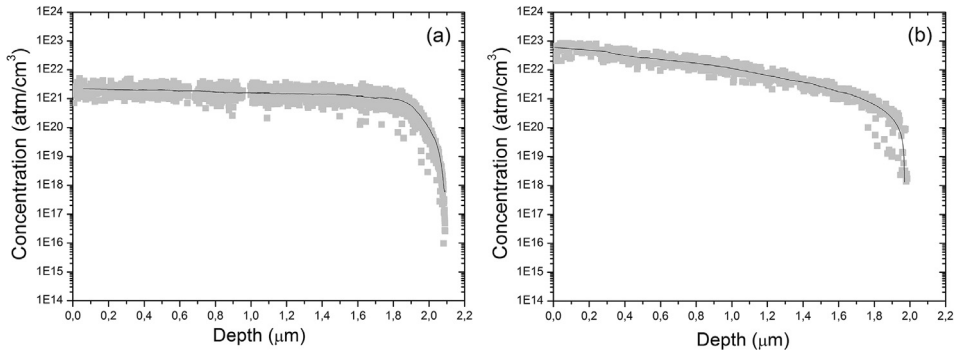

Fig. 4. Deuterium distribution profile in TiD_x samples with (a) low and (b) high concentration of D.

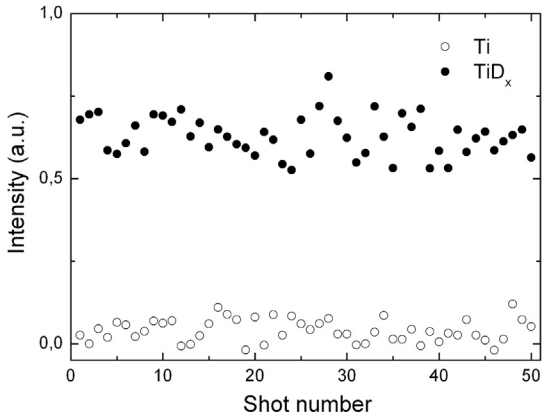

Fig. 5. LIBS 434.40 nm spectrum line intensity of two samples, at the bottom pure Ti and at the top a TiD_x film with a high concentration of deuterium.

concentration of deuterium at the top. In the first one, all peaks correspond to pure Ti in the α (hcp) phase. In the second one, all Ti α reflections have completely disappeared from the TiD_x diffractogram, showing only the reflections corresponding to the δ (fcc) and ϵ (fct) phases, and also other peaks corresponding to the Cu substrate. The Rietveld refinement of the diffraction patterns, shown in Fig. 6(b), estimated a cubic cell parameter $a = (0.4434 \pm 0.0001)$ nm for the δ phase and tetragonal cell parameters $a = (0.4475 \pm 0.0001)$ nm and $c = (0.4379 \pm 0.0001)$ nm for the ϵ phase. These phases are the crystalline structures adopted by the TiH_x system over a concentration range of $1.50 < x < 1.99$ [19,20]. Observing the behavior of the concentration as a function of the lattice parameter, we can estimate the concentration of deuterium (x value) in our samples to be between 1.89 and 1.94 [21,22]. The observed presence of the δ and ϵ phases at room temperature, for these values of deuterium concentration, give an indication of the $\delta/(\delta + \epsilon)$ phase transition.

3.3. Irradiation

All of the titanium deuteride samples were characterized by the previously mentioned techniques, but only those with the higher deuterium concentration were irradiated. As stated before, the titanium deuteride films will be used as neutron production targets, for this purpose, it is necessary that the film withstand ion irradiation as long as possible. Therefore, to evaluate the film resistance, we decided to irradiate it with ion fluences higher than those reported in the literature for titanium deuteride thin films. SEM micrographs of titanium deuteride samples irradiated with fluences of approximately 3×10^{18} ions/cm^2 are shown in Fig. 7. In these figures blisters were found with a mean diameter of 20 μm clearly visible on the surface (a). Most of the observed blisters don't show their blister caps, this indicates surface erosion due to blistering bursts, although a visual inspection of the surface shows that both non bursted (b) and bursted (c) blisters coexist. Also, in Fig. 7(c), can be seen that the bursted blisters creating a hole in the film, exposing the substrate. It is worth mentioning that the bright particles on the surface of each sample are of zinc sulfide, which is the fluorescence material used to determine the incident beam cross section.

Optical profilometry and SEM micrograph were performed in the irradiated samples to evaluate the surface morphology of the titanium deuteride samples (Fig. 8). In 2D surface profile, Fig. 8 (a), it can be seen the bursted and non bursted blisters in the irradiated zone (right-down) and another zone that was not impacted by the beam (left-up). Also, at the irradiated zone, it was observed

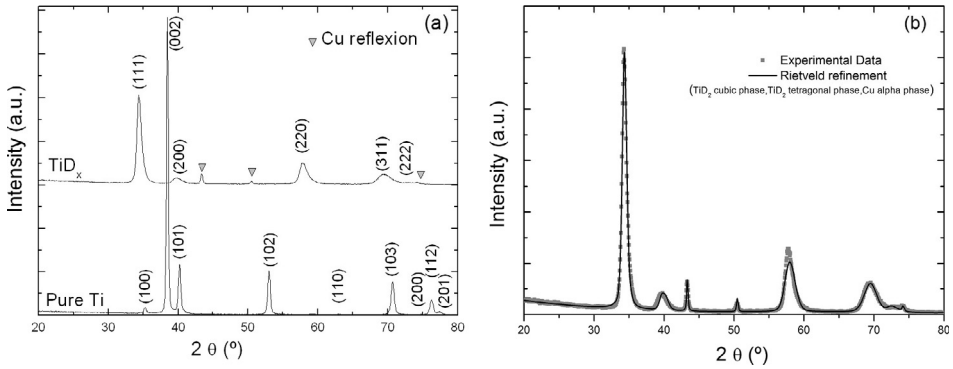

Fig. 6. (a) X-ray diffractograms of pure Ti (α phase) at the bottom and TiD_x samples ($\delta + \epsilon$ phases) at the upper part of the figure. (b) X-ray diffractogram of a TiD_x sample with the result of the Rietveld refinement.

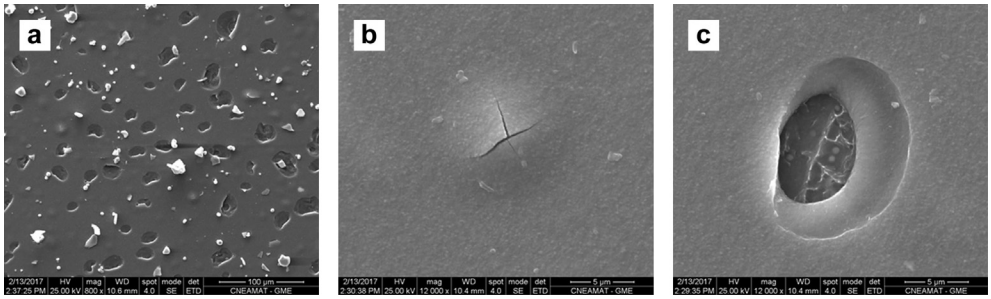

Fig. 7. SEM micrograph of the TiD_x surface sample irradiated with fluences of approximately 3×10^{18} ions/cm^2 (a) surface view, (b) detail of a non bursted blister and (c) detail of a bursted blister.

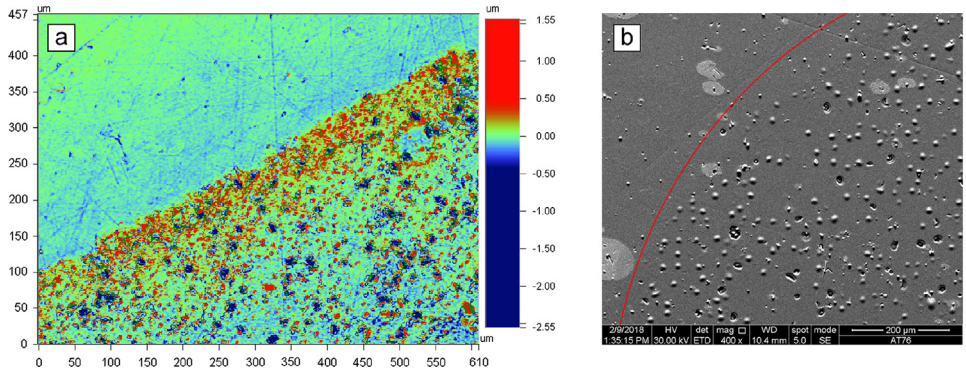

Fig. 8. (a) Optical profilometry and (b) SEM micrograph of the $TiD_{1.89-1.94}$ sample showing the irradiated and non irradiated zone.

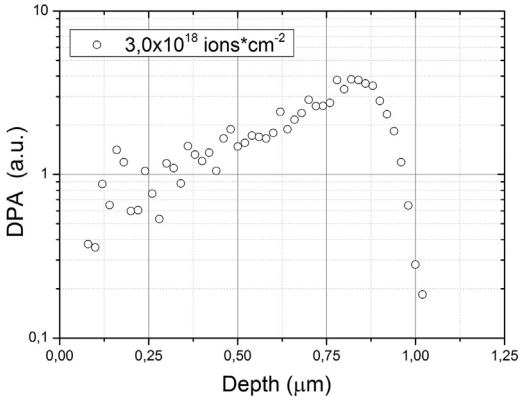

Fig. 9. SRIM simulation of the 150 keV proton beam range, incident on a TiD_2 thin film.

an increase in the surface roughness, where the mean roughness values are two times higher than those of the pristine samples. Fig. 8(b) shows a SEM micrograph of the $TiD_{1.89-1.94}$ sample that included both zones, irradiated (right side) and another zone that was not impacted by the beam (left side). Due to radiation damage by ion bombardment and hydrogen accumulation, at the irradiated zone it could be seen blisters cover a fraction of the surface, with rather large undamaged space between them.

SRIM simulations of the irradiated films allowed us to determine that the incident 150 keV proton beam stops completely at a depth smaller than 1.20 μm and generates a maximum damage of 3.8 DPA, for a fluence of 3×10^{18} ions/cm^2, as can be seen on Fig. 9.

4. Conclusions

Well adhered Ti deposits on Cu and Al substrates, with a mean thickness of 2 μm were produced through PVD. Then, Ti films were impregnated with deuterium under controlled conditions in order to obtain TiD_x samples. Relative deuterium concentrations were evaluated by SEM, ERDA, LIBS and GIRDX, to establish the optimum values for the gas pressure, substrate temperature and exposure time conditions.

In this work, $TiD_{1.89-1.94}$ thin films with high deuterium concentrations were irradiated at the ion injector of the TANDAR accelerator at higher fluences than the ones reported until now in literature, up to 3×10^{18} ions/cm^2. Under the conditions on which these irradiations were carried out, the samples showed blisters over its surface. The observed blisters were well defined, partially or totally eroded. This degradation on the film surface could generate a decrease in the performance of the neutron production target. This means that for some applications, targets would need to be replaced several times a day, depending on current density, due to the damage generated by the injected beam.

Acknowledgments

The authors would like to thank CNEA (National Atomic Energy Commission, Argentine) and CONICET (National Scientific and Technical Research Council, Argentine) for support and funding. They would also like to thank Vittorio Luca and the technical staff responsible for SEM. Martin Alurralde for his helpful collaboration provided during ERDA measurements. Carlos Ararat-Ibarguen for LIBS analyzes. Diego Lamas for his help in characterizing the X-ray diffractograms and the responsible staff to perform the irradiations at TANDAR accelerator.

References

[1] A.J. Kreiner, J. Bergueiro, D. Cartelli, M. Baldo, W. Castell, J. Gomez Asoia, J. Padulo, J.C. Suárez Sandín, M. Igarzabal, J. Erhardt, D. Mercuri, A.A. Valda, D.M. Minsky, M.E. Debray, H.R. Somacal, M.E. Capoulat, M.S. Herrera, M.F. del Grosso, L. Gagetti, M. Suarez Anzorena, N. Canepa, N. Real, M. Gun, H. Tacca, Present status of accelerator-based BNCT, Rep. Pract. Oncol. Radiother. 21 (2016) 95–101.

[2] R.A. Jameson, G.P. Lawrence, C.D. Bowman, Accelerator-driven transmutation technology for incinerating radioactive waste and for advanced application to power production, Nucl. Instrum. Methods Phys. Res., Sect. B 68 (1992) 474–480.

[3] P.K. Nema, Application of accelerators for nuclear systems: accelerator driven system (ads), Energy Proc. 7 (2011) 597–608.

[4] K–N. Leung, J. Reijonen, F. Gicquel, S. Hahto, T–P. Lou, Compact neutron generator development and applications, in: 16th World Conference on NDT, Montreal, Canada, 2004.

[5] International Atomic Energy Agency, Neutron Generators for Analytical Purposes, no. 1 in IAEA Radiation Technology Reports, International Atomic Energy Agency, Vienna, 2012.

[6] A.J. Kreiner, J. Bergueiro, D. Cartelli, W. Castell, J. Gómez Asoia, J. Padulo, J.C. Suarez Sandín, M. Igarzábal, J. Erhardt, D.M. Minsky, A.A. Valda, J.M. Kesque, M. E. Capoulat, M. Herrera, H. Somacal, M.E. Debray, M.F. del Grosso, L. Gagetti, M. Suarez Anzorena, M. Gun, H.E. Tacca, O. Carranza, Development of high power electrostatic accelerators for nuclear and medical purposes in Argentina, Phys. Proc. 60 (2014) 39–44.

[7] L. Gagetti, M.S. Anzorena, A. Bertolo, M. del Grosso, A.J. Kreiner, Proton irradiation of beryllium deposits on different candidate materials to be used as a neutron production target for Accelerator-Based BNCT, Nucl. Instrum. Methods Phys. Res., Sect. A 874 (2017) 28–34.

[8] M. Ohring (Ed.), Materials Science of Thin Films, second ed., Academic Press, San Diego, 2002.

[9] C. Monnin, A. Ballanger, E. Sciora, A. Steinbrunn, P. Alexandre, G. Pelcot, Characterization of deuteride titanium targets used in neutron generators, Nucl. Instrum. Methods Phys. Res., Sect. A 453 (2000) 493–500.

[10] C. Monnin, P. Bach, P.A. Tulle, M. van Rompay, A. Ballanger, Optimisation of the manufacturing process of tritide and deuteride targets used for neutron production, Nucl. Instrum. Methods Phys. Res., Sect. A 480 (2002) 214–222.

[11] L. Meng, H. Tie, Y. Jie, K. Jianlin, L. Jufang, L. Biao, Damage characteristics of TiD_2 films irradiated by a mixed pulsed beam of titanium and hydrogen ions, Plasma Sci. Technol. 18 (2016) 764–767.

[12] J. Liu, Y. Liu, X. Qin, B. Wang, Surface characteristics of titanium deuteride film implanted with deuterium ion beam, Vacuum 99 (2014) 62–67.
[13] C.R. Brune, R.W. Kavanagh, Production and characterization of thin Ti-^{3}H and Ti-^{2}H targets, Nucl. Instrum. Methods Phys. Res., Sect. A 343 (1994) 415–420.
[14] J.P. Greene, H.Y. Lee, H.-W. Becker, Preparation of thin metallic titanium foils as hydrogen targets, Nucl. Instrum. Methods Phys. Res., Sect. A 613 (2010) 462–464.
[15] C. Ararat-Ibarguen, R.A. Pérez, M. Iribarren, Measurements of diffusion coefficients in solids by means of LIBS combined with direct sectioning, Measurement 55 (2014) 571–580.
[16] D.K. Avasthi, W. Assmann, ERDA with swift heavy ions for materials characterization, Curr. Sci. 80 (2001) 1532–1541.
[17] J.F. Ziegler, M.D. Ziegler, J.P. Biersack, SRIM–The stopping and range of ions in matter (2010), Nucl. Instrum. Methods Phys., Res. Sect. B 268 (2010) 1818–1823.
[18] R.E. Stoller, M.B. Toloczko, G.S. Was, A.G. Certain, S. Dwaraknath, F.A. Garner, On the use of SRIM for computing radiation damage exposure, Nucl. Instrum. Methods Phys. Res., Sect. B 310 (2013) 75–80.
[19] R. Checchetto, P. Scardi, Structural characterization of deuterated titanium thin films, J. Mater. Res. 14 (1999) 1969–1976.
[20] I. Lewkowicz, Titanium-hydrogen, Solid State Phenom. 49–50 (1996) 239–280.
[21] R.L. Crane, S.C. Chattoraj, M.B. Strope, A room-temperature polymorphic transition of titanium hydride, J. Less Common Met. 25 (1971) 225–227.
[22] F.D. Manchester, A. San-Martin, Phase Diagrams of Binary Hydrogen Alloys, ASM International, Materials Park, OH, USA, 2000, 238–258.